Atmospheric Pollution Research 15 (2024) 101955

Contents lists available at ScienceDirect

Atmospheric Pollution Research

journal homepage: www.elsevier.com/locate/apr

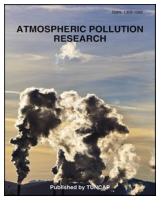

Investigating the reliability of estimating real-time air exchange rates in a building by using airborne particles, including $PM_{1.0}$, $PM_{2.5}$, and PM_{10}: A case study in Suzhou, China

Nuodi Fu [a,f], Moon Keun Kim [b,*], Long Huang [c], Jiying Liu [d], Bing Chen [e], Stephen Sharples [f]

[a] School of Architecture, Southeast University, 2 Sipailou, Nanjing, 210096, China
[b] Department of Built Environment, Oslo Metropolitan University, Oslo, 0130, Norway
[c] School of Intelligent Manufacturing Ecosystem, Xi'an Jiaotong – Liverpool University, Suzhou, 215123 China
[d] School of Thermal Engineering, Shandong Jianzhu University, Jinan, 250101, China
[e] Department of Urban Planning and Design, Xi'an Jiaotong – Liverpool University, Suzhou, 215123, China
[f] School of Architecture, University of Liverpool, Liverpool, L69 7ZX, United Kingdom

ARTICLE INFO

Keywords:
Air exchange rate
Particulate matter
Real-time
Indoor air quality
Outdoor air pollution
Infiltration

ABSTRACT

This study aimed to evaluate the reliability of using airborne particles to estimate the real-time Air Exchange Rate (AER) of buildings, considering particle size and outdoor conditions' impact on the AER estimation accuracy. The study utilized on-site data collection and numerical simulations to analyze the factors affecting the AER prediction accuracy. Results showed that the $PM_{1.0}$- and $PM_{2.5}$-based empirical correlation could predict the AER of buildings with a Normalized Mean Error (NME) of less than 10% and a correlation coefficient (r) of over 0.97, outperforming the pressurization method. Fine particles with a diameter under 2.5 μm were found to be a reliable tracer for AER prediction, with a negative correlation between particle size and AER prediction accuracy due to their higher penetration rate. The study also found that outdoor particle levels and pressure differentials positively impacted the accuracy of PM-based AER estimation. These findings have practical applications for maintaining Indoor Air Quality (IAQ) and accurately predicting a building's heat losses.

1. Introduction and background

Infiltration is the uncontrolled passage of outdoor air through building cracks and ventilation system leakage to enter indoor environments. Under such circumstances, infiltrating air directly brings outdoor air pollutants indoors and significantly degrades Indoor Air Quality (IAQ) (Amphalop et al., 2023; Fattah et al., 2023; Hu et al., 2020; Kim et al., 2022; Li et al., 2019, 2022; Liang et al., 2021; Nazaroff, 2021). Moreover, infiltration can also affect indoor thermal comfort (Goubran et al., 2017; Happle et al., 2017; Mathur and Damle, 2021), ventilation system efficiency (Fu et al., 2021a; Ren et al., 2023a; Ren et al., 2023b; Shi and Li, 2018b), and acoustic insulation performance. Previous studies have reported that a building's heating and cooling loads increase rapidly due to air infiltration (Goubran et al., 2017; Han et al., 2015; Mathur and Damle, 2021). Thus, infiltrating air is undesirable in the case of polluted outdoor air and is also unwanted for low-carbon buildings. Accurately predicting the building's Air Exchange Rate (AER) under natural conditions could help control IAQ and estimate the building's heat loss.

Tracer Gas Methods (TGM) and fan pressurization tests are two widely used techniques for measuring AER. The fan pressurization test involves using fans in doors (blower doors) to pressurize a building to a reference pressure to test its airtightness (CIBSE, 2016). However, the measured AER is idealized under test conditions and ignores the impact of climate variation. Also, a blower door test can only measure the airtightness of a simple building and is limited when applied to large-scale complex buildings, such as high-rise buildings. In reality, the AER varies with actual in-service conditions due to wind pressures and stack effects (Fu et al., 2021a; Nazaroff, 2021; Park et al., 2021; Shi and Li, 2018b, Fu et al., 2022). To obtain a more realistic and dynamic analysis of AER, the variation of AER with climatic conditions is investigated using TGM since it is conducted under actual environmental

Peer review under responsibility of Turkish National Committee for Air Pollution Research and Control.
* Corresponding author.
E-mail addresses: Moon.Kim@oslomet.no, yan1492@gmail.com (M.K. Kim).

https://doi.org/10.1016/j.apr.2023.101955
Received 25 April 2023; Received in revised form 2 October 2023; Accepted 2 October 2023
Available online 8 October 2023
1309-1042/© 2023 Turkish National Committee for Air Pollution Research and Control. Production and hosting by Elsevier B.V. This is an open access article under the CC BY license (http://creativecommons.org/licenses/by/4.0/).

conditions. This method estimates the AER through the building openings based on the decay of a tracer gas's concentration indoors within a selected time period. For precision concerns, the tracer gas should be of outdoor origins or without ambient sources, such as CO, O_3, NO, NO_2, SO_2, and SF_6 (ASTM, 2000; ISO, 2012). Recently, the occupant-generated CO_2 TGM has also been commonly used to assess the room's AER due to its simplicity and not requiring the injection of a tracking gas (Kabirikopaei and Lau, 2020; Park et al., 2021; L. C. Ren et al., 2022; Xiong et al., 2021; Zong et al., 2022).

In recent years, more attention has been paid to assessing AER using indoor and Outdoor Particle Levels (OPL). This method follows the principle that a building is in a steady state, and the amount of air flowing in and out is balanced. Thus, the known inlet and outlet airflow rates can be applied to determine the AER. Serfozo et al. (2014) compared the AER estimation results based on the PM_{10}-based method, which is based on measured PM_{10} mass concentration to predict the air exchange rate, with the CO_2-based method, and they found that the two results showed high agreement with each other. Ni et al. (2017) also successfully predicted the average AER of a test room based on a steady-state indoor $PM_{2.5}$ level, with AER results determined by the CO_2 decay method also being used as the baseline.

Moreover, two new methods have been developed to measure the air exchange rate of a room using particulate matter (PM) as a proxy. These are the $PM_{2.5}$-based Clean Air Delivery Rate (CADR) method and the $PM_{2.5}$-based PM-up method. Liu et al. (2021) justified that the developed CADR method is feasible to replace the CO_2 decay method to measure the building's AER. The method involves using a portable air purifier to analyze the dynamic process of indoor particle levels and fitting the data to a numerical model to predict the average AER. Further, the PM-up method has been developed by Hu et al. (2022) to overcome the disturbance created by normal human indoor activities to ensure the AER could be measured accurately. The central highlighted point in this study was that they created a bounce-up process of indoor fine particles level by turning on the air cleaner at the beginning and then turning it off, which makes the IPL increased rapidly in a short period. During the bounce-up process, the source of indoor fine particles level is only outdoor particles because of air change with the outdoor air. Thus, the average AER of the tested room can be determined by fitting the measured Indoor Particle Level (IPL) in that period with the numerical model, and the estimated results' accuracy has been analyzed by comparing it with CO_2 decay methods (Hu et al., 2022).

Previous research has focused on predicting the average AER of a room, but this may not accurately reflect the indoor air quality (IAQ) and heating loss of a building. Real-time AER measurements are required to better control IAQ and predict actual heat loss. However, there is limited research on using airborne particles to estimate real-time AER, and particle size has been found to significantly impact the accuracy of the estimation. (Shi et al., 2017). This is because the larger particles are easier to lose due to the deposition and resuspended mechanism and more difficult to penetrate through building cracks (Lai and Nazaroff, 2000; Qian and Ferro, 2008; Serfozo et al., 2014; Zhao and Wu, 2007). Hence, it is expected that the accuracy of the PM-based AER estimation method is highly correlated to particle size. However, most previous research only explored the possibility of predicting the AER of a room based on one size of particles. Therefore, new research is required to compare the accuracy of estimating AER based on different particle sizes, including $PM_{1.0}$, $PM_{2.5}$ and PM_{10}, under various outdoor conditions. Existing literature (Gomes et al., 2007; Isiugo et al., 2019; Martins & Carrilho da Graça, 2018; Stamp et al., 2022; Yang et al., 2015) suggests that indoor particles can be influenced by various factors, including occupant activities, dust type, dust load, indoor floor type, and humidity. However, this study specifically concentrates on determining the accuracy of real-time air exchange rate estimation using airborne particles in unoccupied rooms. Assessing how outdoor air pollution levels can impact indoor air pollution levels in occupied rooms is limited due to the significant influence of dynamic behaviors, occupant activities, and floor material types on indoor airborne particle levels.

This study aimed to explore the impact of particle size on real-time AER assessment using the particles' mass balance method, while accounting for different outdoor conditions. The study demonstrates the potential of using airborne particles mass concentration differences between indoor and outdoor conditions to estimate AER, particularly in a building where traditional methods may be challenging to apply. The results can inform the reliability of airborne particles in predicting real-time AER and help accurately estimate indoor pollution rates and building heat loss. Literature has described estimating indoor particle concentrations of outdoor air pollution origin (Diapouli et al., 2013; Diapouli et al., 2007; Meng et al., 2005; C. L. Ren et al., 2022; Rojas--Bracho et al., 2004; Wang et al., 2023; Wichmann et al., 2010). The research specifically investigated the influence of particle size and outdoor conditions on the accuracy of AER real-time estimation. The study incorporated PM1.0, PM 2.5 and PM 10 and considered various boundary conditions, such as the summer season, stack effect, temperature and humidity differences using real time data to determine the pressure drop in relatively low air pollution season. While the penetration factors align with the reference values which the ranges are quite broad and not reflected by real time scenario, it's important to note that the actual infiltration rate of particles (PM1.0, PM2.5, and PM10.0) can be influenced by real time factors.

2. Methodology

The methodologies used to analyze the accuracy of estimating AER based on the airborne particles' mass balance method can be divided into five steps: 1) Collecting on-site data of both indoor and outdoor particle levels; 2) A numerical model is established to fit the measured IPL based on the mass balance equation; 3) Analyzing the collected data using the established model; 4) Develop empirical correlation based on the collected data to determine the real-time AER; 5) The empirical correlation is validated using the K-fold cross-validation method.

2.1. The tested building

The study was conducted in a naturally ventilated 12-floor building located in Suzhou, Jiangsu Province, China. The building is around 63 m high and faces north-south. The experiment was conducted in a room on the building's 3rd floor, which is 10.4 m above the ground floor, and it is situated north of the building. The reason for choosing 3rd floor as the experiment site was that the ground floor sometimes will be the temporary parking area, which may short-term affect the monitoring data and further impact the accuracy of the results. Fig. 1 provides detailed information on the tested building and room. Additionally, the building is surrounded by pedestrian and vehicle roads on a relatively open site.

2.2. Blower door test

According to the standard EN 13829 (CEN, 2001), the pressurization method is suggested to assess a room's airtightness and this method has also been successfully applied in previous research (Ji and Duanmu, 2017a, 2017b; Ji et al., 2017, 2020). Hence, the pressurization method was used to determine the tested room's airtightness, and experiments were performed strictly with the standard. The Retrotec 5000 system, as shown in Fig. 2, which consists of a Model 5000 fan, a cloth panel, and a control panel. The cloth panel is used to seal the opening and set the rest part of the system, the fan is used to pressurize and depressurize the test room at the required airflow rates, and the 32-DM digital manometer control device is applied to control the whole system.

Ten tests were done to assess the selected room's AER to minimize the measurement error, and test results varied within a range of ±5%. Then the average of the results was utilized in this study and is displayed in Table 1. ASHRAE Handbook (ASHRAE, 2017) reported that a room's AER is a function of the pressure differential, which is shown below:

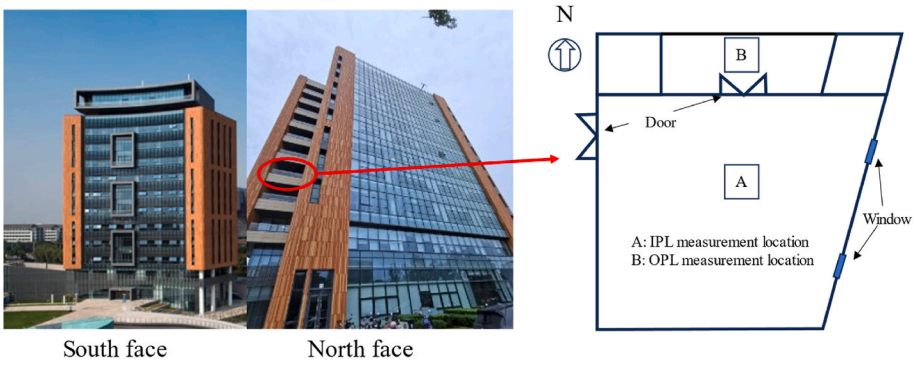

Fig. 1. The target building and test room.

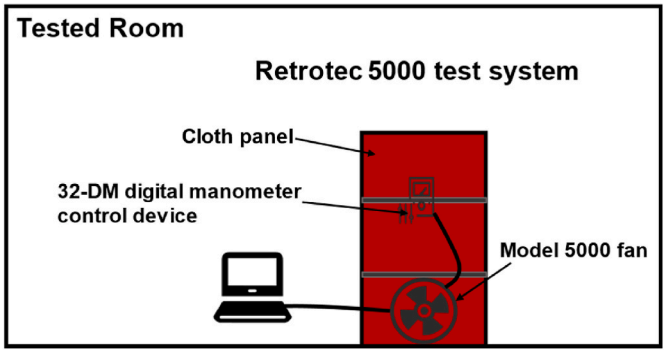

Fig. 2. The Retrotec 5000 test system.

Table 1
The chosen room's airtightness test results.

Air flow coefficient (m^3/(h*Pa)	Air exchange rate at 50 Pa (h^{-1})	ELA at 50Pa (cm^2)	ELA per envelope area at 50Pa (cm^2/m^2)	Slope, n
24.8	8.3	25.3	2.1	0.597

$$AER = \frac{3600}{V} \times c \times (\Delta p)^n \quad (1)$$

where AER is the air exchange rate due to the infiltrated air in h^{-1}, and V is the room's volume in m^3. According to Table 1, the mean value of the exponent n and the airflow coefficient, c, in $m^3/(s{\cdot}Pa^n)$ was calculated and applied. Thus, based on the results of blower door tests, Equation (1) can be rewritten as:

$$AER = 0.146 \times (\Delta p)^{0.597} \quad (2)$$

Equation (2) shows the correlation between the AER of the selected room and the pressure differential. Moreover, a manometer was used to assess the pressure differential during experiments, and results were applied to Equation (2) to determine the real-time AER of the room.

2.3. Design of experiments

The on-site measurements were conducted from June 1st to June 11th, 2022 in a trapezoidal-shaped room that was naturally ventilated without mechanical ventilation system. The doors, windows, and any obvious leaks were sealed during the experiment to ensure that particles could only enter through infiltrated air through building cracks. Each experiment lasted for 245 min to reach a steady state of IPL. Based on the results of the pilot study before the official experiment, the first 5 min of measured data were excluded from the data analysis to avoid any influence from people's movements on the final results.

During the experiments, indoor and outdoor particle levels were simultaneously collected, with all instruments calibrated before each experiment according to the manufacturer's handbook. Tables A and B (shown in right part of Fig. 1) were used to place the calibrated instruments to collect data. Table A was situated in the middle of the room, while table B was on the room's balcony, 1.5 m away from the room, and both tables were 0.9 m above the floor. The monitors collected one piece of data every 10 s and recorded the average value of the collected data every minute.

2.4. Instrumentation

This study utilized TSI DustTrak Aerosol monitors (Model 8534) to measure the concentrations of indoor and outdoor particles. These monitors are handheld instruments that use the 90° light scattering technique, which means that the volume concentration of aerosols is directly proportional to the amount of scattered light. This instrument has been used in several widely accepted papers to measure atmospheric particles (Fu et al., 2021a, 2021b; Liu et al., 2018; Wu et al., 2002). Additionally, the manufacturer calibrated the instruments using the Arizona Test Dust before conducting the experiments. Table 2 provides a summary of the testing instruments, including their manufacturer-reported accuracy, resolution, and detection range.

2.5. Indoor particles' mass balance model

The indoor particle level is a function of source (S_i) and loss terms (L_i), which the equation could describe as (Ben-David and Waring, 2016; Fu et al., 2021a, 2021b; Kim and Choi, 2019; Liu et al., 2021; Serfozo et al., 2014):

$$\frac{dPM_{in,t}}{dt} = S_i - L_i \times PM_{in,t} \quad (3)$$

where $PM_{in,t}$ is the indoor particle level at time t in $\mu g/m^3$. Because experiments were conducted in an office room, and thus the emission sources of indoor PM were neglected (EPA, 2019), and the particles were uniformly distributed indoors (Huang et al., 2017). Therefore, the indoor particles are entirely from the outdoor particles that penetrate the building with the infiltration air. Moreover, the particle resuspension rate due to human activities can be ignored in a steady-state indoor condition compared with the deposition rate (Shi and Li, 2018a), and thus, Equation (3) can be described as:

$$\frac{dPM_{in,t}}{dt} = p \times Q \times PM_{out,t} - (Q + \beta) \times PM_{in,t} \quad (4)$$

where p is the penetration factor of the particle (no units), Q is the AER of the building in h^{-1}, $PM_{out,t}$ is the outdoor particle level at time t in $\mu g/m^3$, and β is the deposition rate in h^{-1}. Equation (5) is the dynamic solution of Equation (4), which illustrates the indoor PM level (Diapouli

Table 2
Detailed information regarding the utilized instruments.

Parameter	Instrument	Range	Accuracy	Resolution
Pressure differential	Vadias QDF70A-VD-S	±100 Pa	0.5% FS	0.1 Pa
$PM_{1.0}$	TSI Model 8534 DustTrak	0.001–150 mg/m^3	1 μg/m^3 or ±0.1% of the reading	0.1–15 μm
$PM_{2.5}$				
PM_{10}				
Air temperature	Testo 635-2	−60 – 400 °C	0.1 °C or ±0.3 °C of reading	0.1 °C

et al., 2013; Quang et al., 2013; Ruan and Rim, 2019; Yu et al., 2014).

$$PM_{in,t} = \frac{p \times Q}{Q+\beta} \times PM_{out,t} + \left(PM_{in,0} - \frac{p \times Q}{Q+\beta} \times PM_{out,t} \right) \times e^{-(Q+\beta)\times t} \quad (5)$$

Then, the equation can be rewritten as:

$$PM_{in,t} = a + b \times e^{-c \times t} \quad (6)$$

hence, the decay of the IPL should be shown as an exponential curve along with the time. According to previous studies, it is reasonable to assume that these coefficients, including p, Q, and β, are constant within a short time slot, such as 1 h (Sun et al., 2019; Xiang et al., 2021). Table 3 presents the input values for each particle's penetration and deposition rate. Further, by substituting the measured OPL and these factors into Equation (5), the IPL can be estimated. The comparison between measured and estimated IPL can illustrate the possibility of using airborne particles to predict the AER of a building.

2.6. Method assessing index

To assess the comparison of different sizes of the PM-based method with the pressurization method and the comparison of two different PM-based methods with the pressurization method, two statistical indices are introduced, the Normalized Mean Error (NME) and the correlation coefficient (r) (Liu et al., 2021).

NME evaluates models by observation, ensuring the results in a relative sense. Moreover, NME is calculated by characterizing the average model error's magnitude on a spatiotemporal scale. Accordingly, the small NME indicates the consistency of the two assessing methods, and 30% was chosen as the baseline for NME evaluation in this study (Liu et al., 2021). The NME can be defined as:

$$NME = \frac{\sum |P_i - O_i|}{\sum O_i} \quad (7)$$

where P_i and O_i are the air exchange rate estimated by the PM-based and pressurization methods in h^{-1}. Further, the correlation coefficient is used to assess the variability of two compared methods in an entire range, and the closer that r is to unity, the better the agreement between the two methods (Liu et al., 2021). In this study, the baseline value of r is set to 0.4, and it can be defined as:

$$r = \frac{\sum [(P_i - \overline{P})(O_i - \overline{O})]}{\sqrt{\sum (P_i - \overline{P})^2} \sqrt{\sum (O_i - \overline{O})^2}} \quad (8)$$

where $\overline{P}$ and $\overline{O}$ are the mean values of the AER in h^{-1} estimated by PM-based and pressurization methods, respectively.

Table 3
The input value for each particle's penetration and deposition rate (He et al., 2005).

Factors	$PM_{1.0}$	$PM_{2.5}$	PM_{10}
Penetration rate (–)	0.9	0.8	0.63
Deposition rate (h^{-1})	0.14	0.31	0.7

3. Results and discussion

3.1. Measured indoor particle level

The analysis conducted in this study revealed that the IPL would undergo exponential decay in the absence of indoor emission sources. To model the measured IPL, Equation (6) was used, and Figs. 4-6 depict the measured IPL along with the fitted curve for each particle type, using data collected on June 1st as an example. In addition, Fig. 3 presents the outdoor conditions recorded during the data collection period, which lasted from 8 a.m. to 12 a.m (see Fig. 4).

From Fig. 3, it is evident that outdoor particle concentrations followed a consistent trend throughout the day, with higher levels observed in the morning and lower levels in the afternoon. This trend indicates a negative correlation between the OPL and outdoor air temperature on a daily basis, a pattern that is also observed during seasonal changes. For instance, OPL was higher in winter and lower in summer (Fu et al., 2021a, 2021b). The measured data indicated that PM_{10} levels outdoors in Suzhou were generally the highest, followed by fine and very fine particles. Additionally, the temperature differential initially decreased and then increased during the experiments. This occurred because the experiments commenced at 8:00 in the morning, resulting in lower indoor air temperature due to night cooling, which led to a higher temperature differential initially.

Upon analysing Figs. 4-6, a strong correlation between the measured and fitted indoor particle levels was observed, with the coefficient of determination (R^2) consistently exceeding 0.99. In other experiments, R^2 ranged from 0.992 to 0.999. As mentioned earlier, PM_{10} levels were typically the highest among the three selected particle sizes, both indoors and outdoors under steady-state conditions. This indicates a strong correlation between indoor and outdoor particle levels. Moreover, the graphs demonstrated that even in the absence of indoor emission sources, the Indoor-to-Outdoor (I/O) ratio of particles could reach 3–5. This is because indoor air can become contaminated if the room has not been used for a while (EPA, 2019).

3.2. The impact of particle size on the accuracy of estimating real-time AER

A study was conducted to compare the measured and estimated IPL to investigate the reliability of using airborne particles to predict the AER of a building, and the results are shown in Figs. 7-9. According to the graphs, predicting the AER based on the smaller particles is generally more accurate than for the larger ones. This is because $PM_{1.0}$ and $PM_{2.5}$ have a smaller size and higher penetration rate, making it easier for them to enter the room with the infiltrated air. Thus, the result of the estimated AER based on the small particle is closer to the real AER. Then, the estimated indoor PM_{10} concentration is always lower than the measured one. Hence, the PM_{10}-based predicted AER is easily underestimated, and the results are highly agreed with previous studies (Sun et al., 2019; Xiang et al., 2021), i.e. that the larger particle has a higher deposition rate and lower penetration rate, which highly impacts on its ability to get in or out of the room.

The lower bound of the estimated IPL is lower than the measured ones when the IPL reaches a steady state, as shown in Fig. 10. This indicates that the actual IPL is higher than expected, and using a steady-

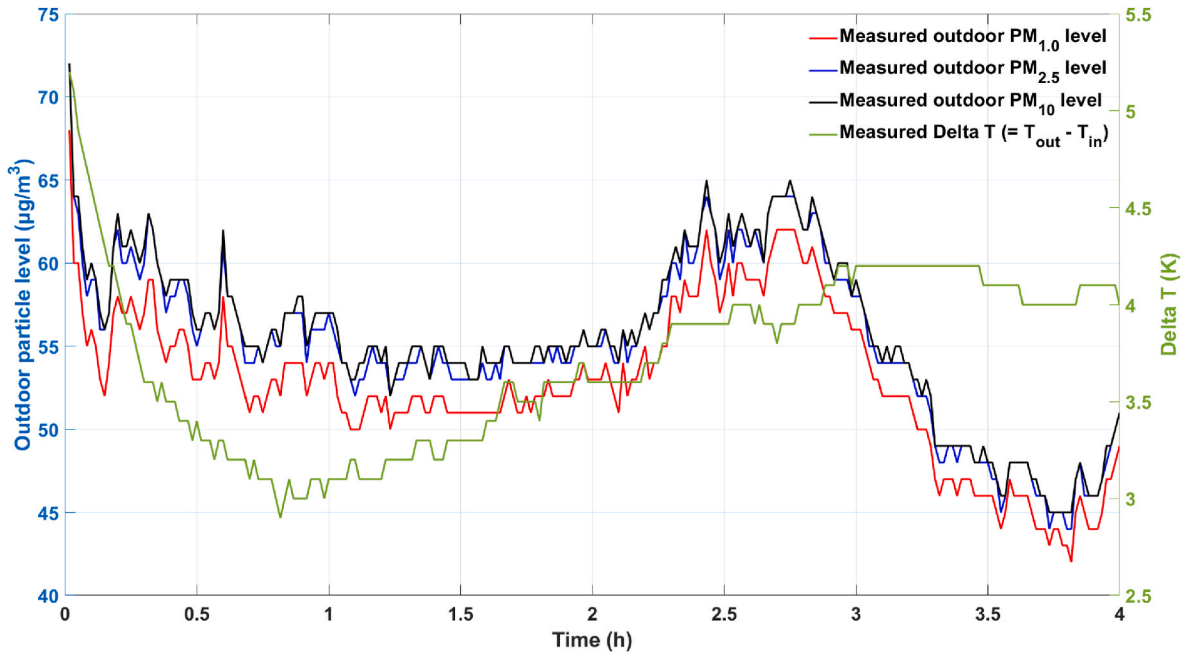

Fig. 3. The outdoor particle level on the selected day (01/06/2022) and the temperature differential in the selected room (the experiment duration is from 8:00 a.m. to 12:00am).

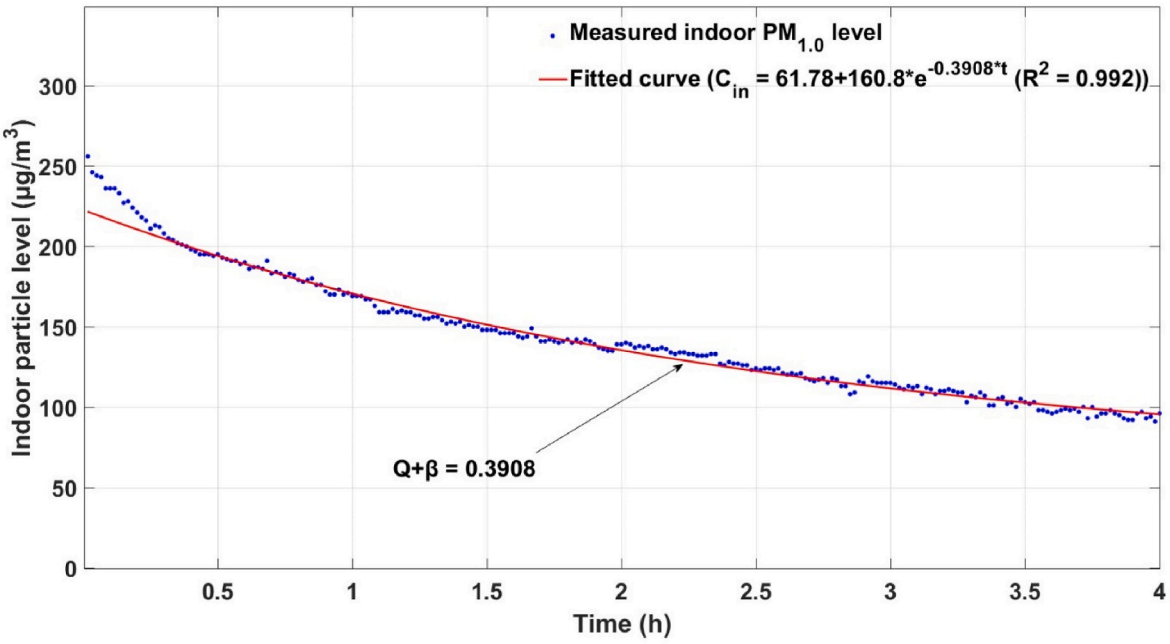

Fig. 4. The measured and fitted curve of indoor $PM_{1.0}$ on the 1st of June (the experiment duration is from 8:00 a.m. to 12:00am).

state IPL to predict AER can lead to an increased error and underestimation of results. This phenomenon is more notable as the particle size increases. Table 4 presents the results using two selected statistical indices to evaluate the comparison of estimated and measured IPL. The results show that estimating AER based on smaller particles, such as $PM_{1.0}$ and $PM_{2.5}$, is more accurate than using larger particles such as PM_{10}. The error between estimated and measured indoor $PM_{1.0}$ levels varied from 9.41% to 18.32%, which is below the criterion value of 30%. The NME value for $PM_{2.5}$ sometimes did not meet the criteria but was generally acceptable, while for PM_{10}, the NME value was significantly over the standard value.

The correlation coefficient (r) value was at least over 0.87, indicating that the estimated IPL had a better agreement in variability over the entire range of the measured one. Based on the data analysis, using $PM_{1.0}$ and $PM_{2.5}$ as tracers is suggested to predict the real-time AER of a building.

3.3. The impact of outdoor conditions on the accuracy of estimating real-time AER

The IPL of a building depends on the OPL and AER, which is influenced by the pressure differential. It's reasonable to assume that the accuracy of estimating IPL is affected by these two factors. Therefore, this study used Spearman's rank correlation coefficient ρ to evaluate the

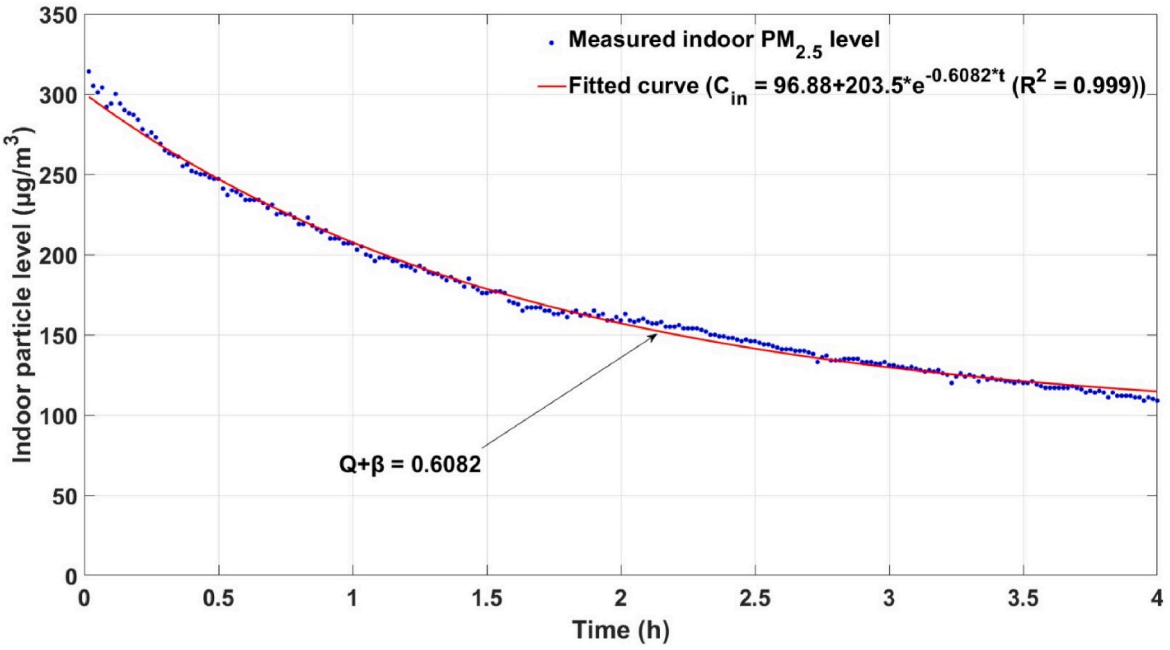

Fig. 5. The measured and fitted curve of indoor $PM_{2.5}$ on the 1st of June (the experiment duration is from 8:00 a.m. to 12:00am).

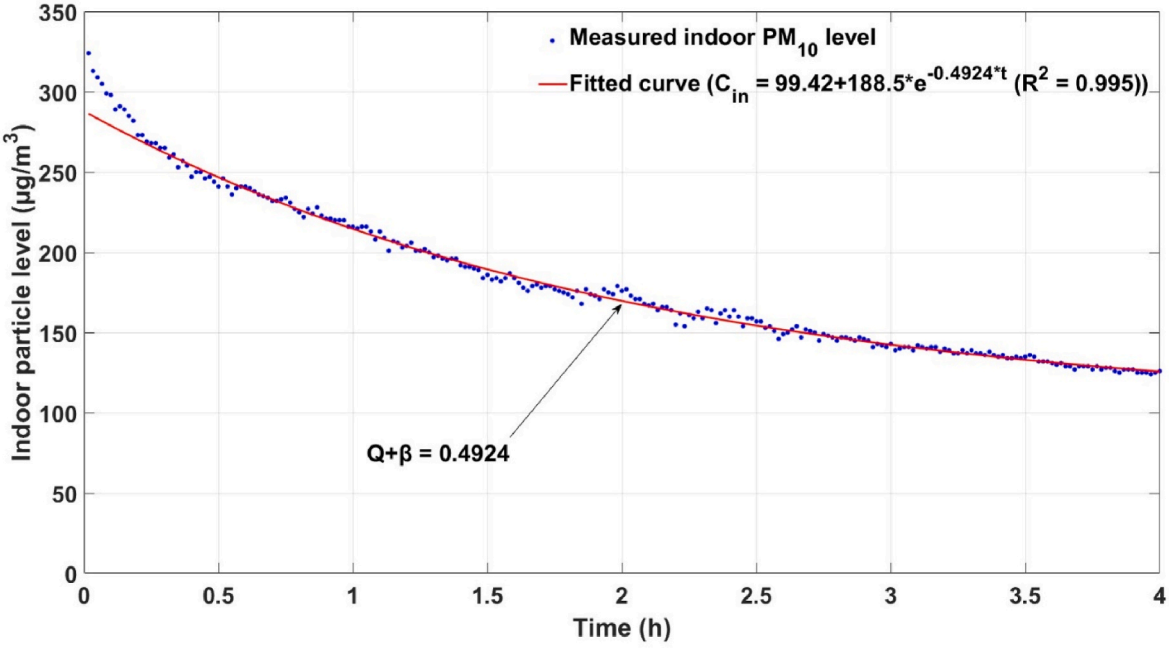

Fig. 6. The measured and fitted curve of indoor PM_{10} on the 1st of June (the experiment duration is from 8:00 a.m. to 12:00am).

correlation between the Normalized Mean Error (NME), representing the error between measured and estimated IPL, and the OPL and pressure differential. The instantaneous NME was compared with the measured OPL and pressure differential, and the results are presented in Table 5. The analysis showed that the OPL and pressure differential significantly influence the predicting accuracy of the IPL and also affect the accuracy of predicting AER.

From Tables 4 and 5, the results suggest that the accuracy of estimating AER will increase when the I/O ratio of particles increases, particularly for larger particles, as the ρ value for Day 1 to Day 6 is closer to unity, and p value is kept smaller than 0.001. However, this trend was not observed when the OPL was extremely low, as on Day 7, and the impact was more significant on larger particles than smaller ones. From Table 4, the findings on Day 7 indicate that the estimated indoor $PM_{2.5}$ and PM_{10} levels were discrepant from the actual values, with an NME value exceeding the baseline value of 30%, while the NME value for $PM_{1.0}$ was only around 10%. The results suggest that the $PM_{1.0}$-based method can still provide acceptable performance in predicting AER when the OPL is extremely low. One possible reason is that outdoor $PM_{1.0}$ is the dominant source of indoor $PM_{1.0}$ particles in a building with no cooking allowed (Lee et al., 2006). For indoor $PM_{2.5}$ and PM_{10}, the low outdoor level may reduce their impact, resulting in the IPL being affected by other factors such as resuspension and deposition mechanisms (Stratigou et al., 2020).

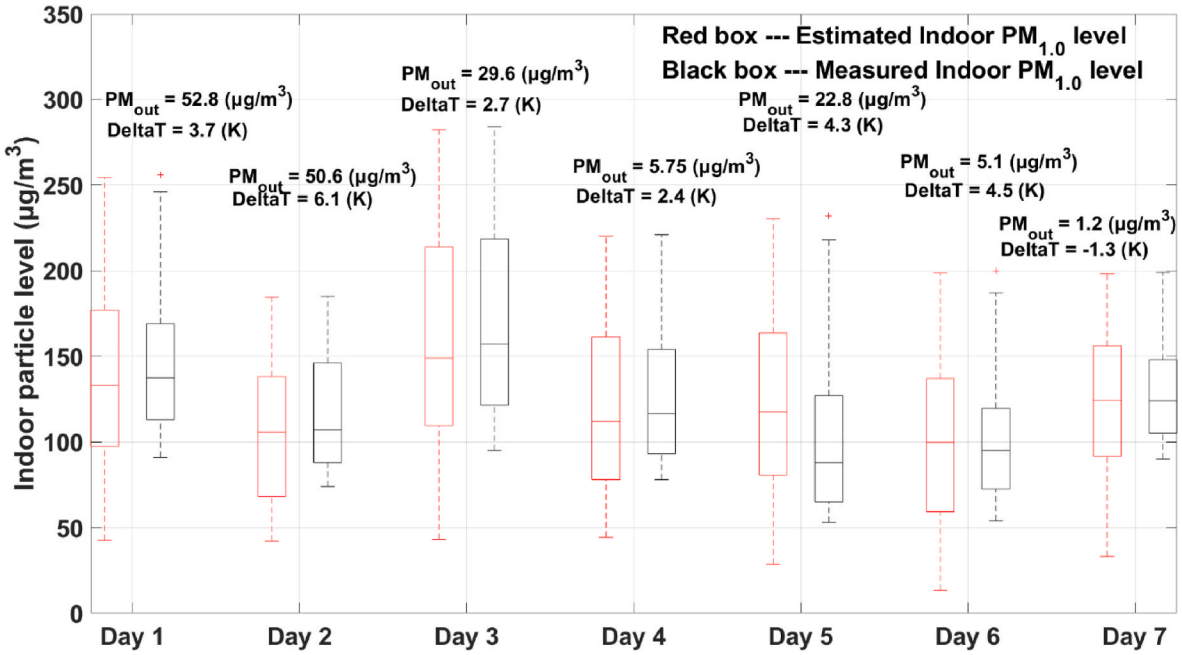

Fig. 7. The measured and predicted indoor $PM_{1.0}$ concentration (For each box, the five values are the minimum value, first quartile, Median value, third quartile, and maximum value).

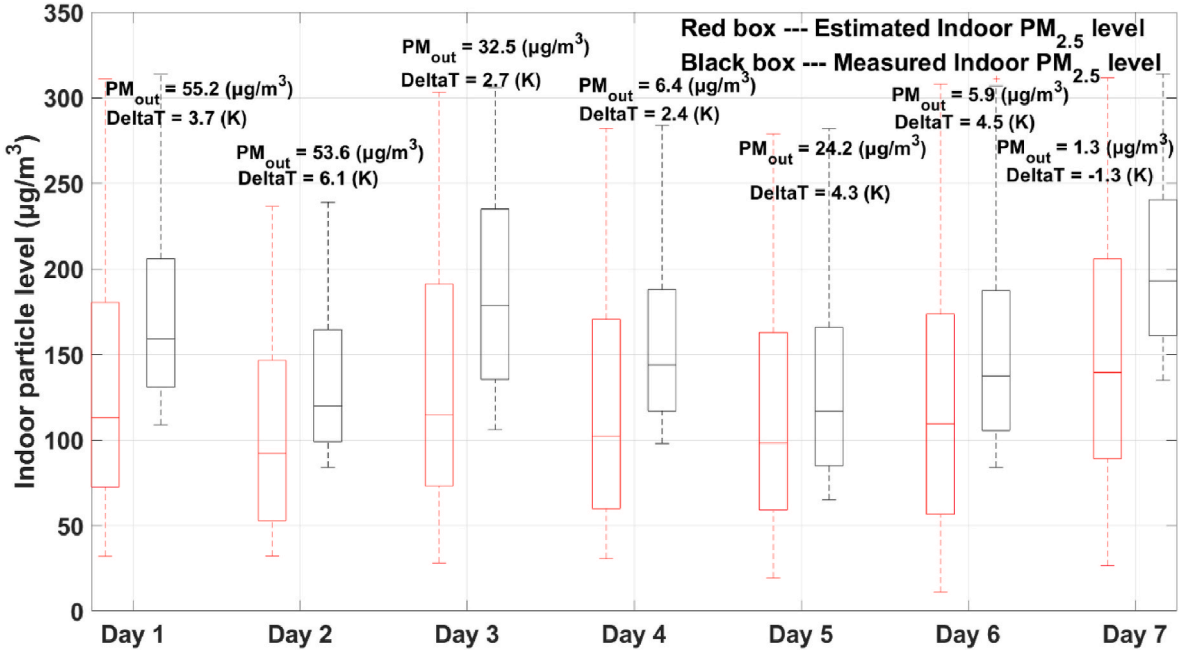

Fig. 8. The measured and predicted indoor $PM_{2.5}$ concentration (For each box, the five values are the minimum value, first quartile, Median value, third quartile, and maximum value).

Additionally, the pressure differential has a positive impact on the accuracy of estimating IPL and predicting AER based on airborne particles. The significance of the pressure differential's negative impact is lower than that of the I/O ratio's impact, as the ρ value is small. Based on the results, the impact of pressure differential is more substantial on the accuracy of estimating smaller particles' IPL since the ρ value decreases when particle size increases. The pressure differential consists mainly of stack-effect and wind-effect. However, the measured IPL has not followed the variation of the measured pressure differential, and its fluctuation is better fitted with the temperature differential (as shown in Fig. 10). The results suggest that the wind effect's impact on the IPL can be neglected, which is in agreement with the previous finding that the stack effect is the dominant force driving the high-rise building's AER (Fu et al., 2021b).

Overall, both factors, I/O ratio and pressure differential, negatively impact the NME between measured and estimated IPL, indicating that both factors positively impact estimating IPL and predicting AER based on airborne particles. Furthermore, the I/O ratio has a more significant impact on larger particles, while the pressure differential has a more notable impact on smaller particles. However, considering all factors, particles with sizes smaller than 2.5 μm are suggested as a tracer to predict the AER of a building.

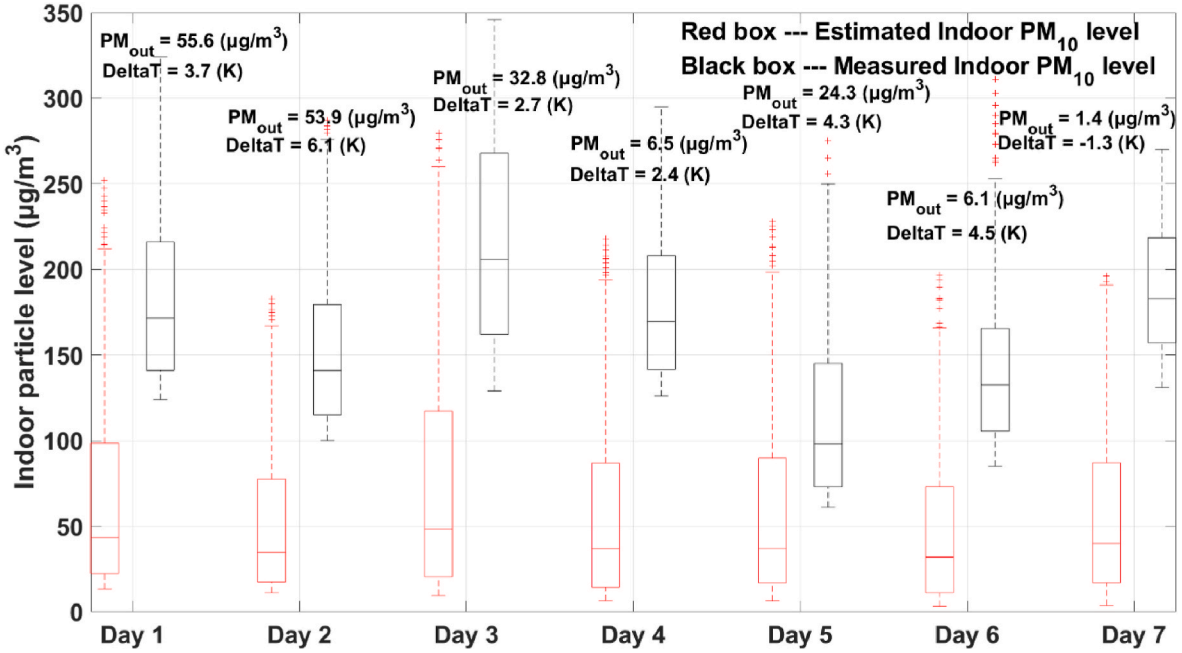

Fig. 9. The measured and predicted indoor PM_{10} concentration (For each box, the five values are the minimum value, first quartile, Median value, third quartile, and maximum value).

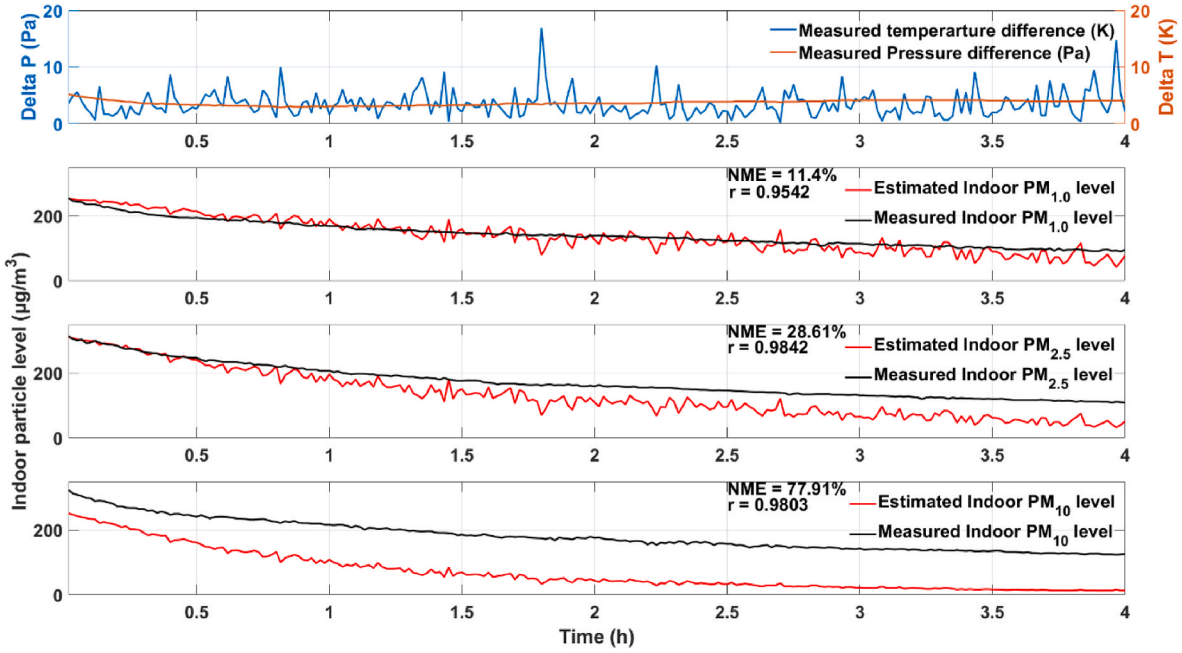

Fig. 10. Time-varied estimated and measured IPL, selected the 1st of June as an example.

3.4. *The empirical correlation for predicting the air exchange rate*

As discussed, particle size, I/O ratio, and pressure differential have a significant impact on estimating the IPL and predicting the AER based on airborne particles. The pressure difference is the main driving force behind AER and also affects the IPL. A function was developed that incorporates the pressure differential and particles' I/O ratio to describe the AER of the building. It is important to note that the data collected on Day 7 was excluded from establishing the numerical model due to its inaccuracy, as determined by the analysis. Furthermore, the I/O ratios of $PM_{1.0}$ and $PM_{2.5}$ were used to establish the numerical model because the method of estimating AER based on PM10 has been found to be less accurate. The numerical model was constructed based on the AER determined by the measured I/O ratios of $PM_{1.0}$ and $PM_{2.5}$, as well as the measured pressure differential. Detailed information regarding this can be found in Figs. 12 and 13. Additionally, empirical correlations based on the experimental data are presented in Equations (9) and (10).

$$\text{For } PM_{1.0}: AER = 0.112 + 0.05305 \times |\Delta P| - 0.002567 \times \frac{I}{O} + 0.000918 \times |\Delta P| \times \frac{I}{O} + 5.635 \times 10^{-5} \times \frac{I^2}{O} - 1.713 \times 10^{-5} \times |\Delta P| \times \frac{I^2}{O} - 2.108 \times 10^{-7} \times \frac{I^3}{O} \quad (R^2 = 0.9891) \tag{9}$$

Table 4
The accuracy analysis of using airborne particles to estimate the real-time AER.

		Outdoor level (μg/m^3)	ΔT (K)	NME (%)	r
Day 1	$PM_{1.0}$	52.8 (42–68)[1]	3.7 (2.9–5.2)[2]	11.4	0.9542
	$PM_{2.5}$	55.2 (44–72)		28.61	0.9842
	PM_{10}	55.6 (45–72)		77.91	0.9803
Day 2	$PM_{1.0}$	50.6 (41–65)	6.1 (5.6–8.5)	9.41	0.9564
	$PM_{2.5}$	53.6 (42–70)		19.88	0.9824
	PM_{10}	53.9 (43–71)		68	0.9834
Day 3	$PM_{1.0}$	29.6 (22–34)	2.7 (1.8–3.2)	14.98	0.9223
	$PM_{2.5}$	32.5 (24–39)		38.17	0.9611
	PM_{10}	32.8 (24–39)		96.62	0.9502
Day 4	$PM_{1.0}$	5.75 (2–10)	2.4 (1.5–4.7)	11.4	0.9392
	$PM_{2.5}$	6.4 (3–11)		26.28	0.9717
	PM_{10}	6.5 (3–11)		81.26	0.9585
Day 5	$PM_{1.0}$	22.8 (16–39)	4.3 (3–8.6)	18.32	0.9013
	$PM_{2.5}$	24.2 (17–42)		15.28	0.9637
	PM_{10}	24.3 (17–42)		35.05	0.9815
Day 6	$PM_{1.0}$	5.1 (3–7)	4.5 (3.5–6.6)	13.99	0.8716
	$PM_{2.5}$	5.9 (4–9)		25.23	0.9459
	PM_{10}	6.1 (4–9)		64.93	0.9782
Day 7	$PM_{1.0}$	1.2 (1–4)	−1.3 (−2.5 – 0.2)	9.82	0.9082
	$PM_{2.5}$	1.3 (1–4)		35.42	0.9756
	PM_{10}	1.4 (1–5)		89.3	0.9563

Hint: 1. The value in the parentheses represents the minimum and maximum OPL during the experiments.
2. The value in the parentheses represents the minimum and maximum pressured differential during the experiments.

Table 5
The results of the correlation analysis based on Spearman's rank correlation coefficient for ranked data.

NME value	Date	I/O ratio	Delta P
$PM_{1.0}$	Day 7	$\rho = -0.2917$; $p < 0.001$	$\rho = -0.2743$; $p < 0.001$
$PM_{2.5}$	Day 7	$\rho = -0.0305$; $p < 0.05$	$\rho = -0.3247$; $p < 0.001$
PM_{10}	Day 7	$\rho = 0.2025$; $p < 0.05$	$\rho = -0.1707$; $p < 0.001$

$$\text{For } PM_{2.5}: AER = 0.1101 + 0.05332 \times |\Delta P| - 0.001842 \times \frac{I}{O} + 0.0007822 \times |\Delta P| \times \frac{I}{O} + 2.419 \times 10^{-5} \times \frac{I^2}{O} - 1.206 \times 10^{-5} \times |\Delta P| \times \frac{I^2}{O} + 4.524 \times 10^{-8} \times \frac{I^3}{O} \quad (R^2 = 0.9891) \tag{10}$$

where AER is the air exchange rate in h^{-1}, ΔP is the pressure differential in Pa, and $\frac{I}{O}$ is the indoor/outdoor particles level's ratio, no units.

Upon examining Figs. 11 and 12, it becomes apparent that the fitted model experienced errors at certain discrete points. Upon analysing the input data, it was observed that these discrete data points were primarily collected during a period when the IPL had not yet reached a steady state. This occurrence could be attributed to the initial variation in the pressure differential between the indoor and outdoor environments, which led to rapid fluctuations in the IPL. Furthermore, in order to validate the developed numerical model, a 5-fold Cross-Validation approach was employed. the prediction accuracy exhibits a slight decrease over time. As depicted in Fig. 12, the difference between the measured and estimated values gradually increases with time. Notably, this phenomenon becomes more pronounced as the particle size increases.

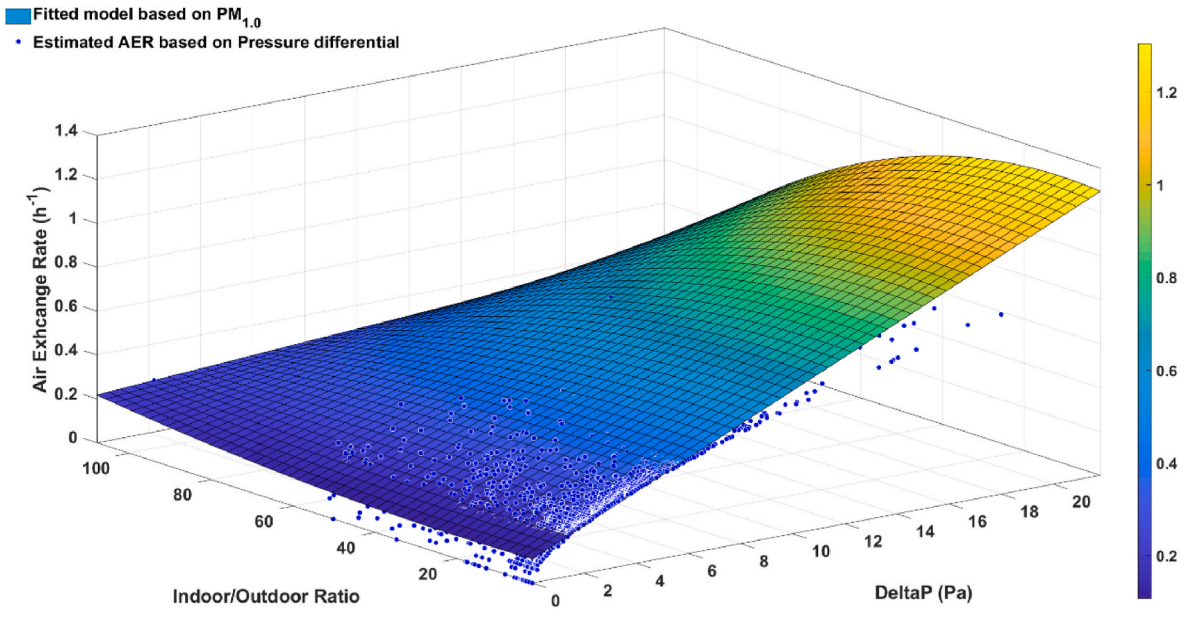

Fig. 11. The fitted model of AER based on $PM_{1.0}$'s I/O ratio and pressure differential.

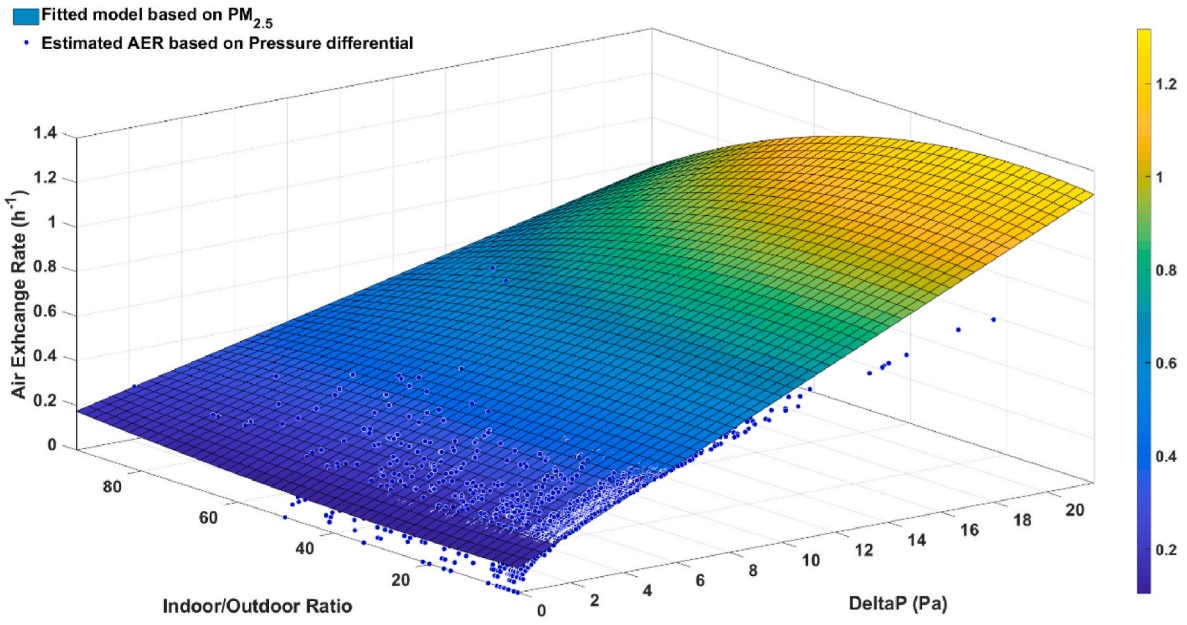

Fig. 12. The fitted model of AER based on $PM_{2.5}$'s I/O ratio and pressure differential.

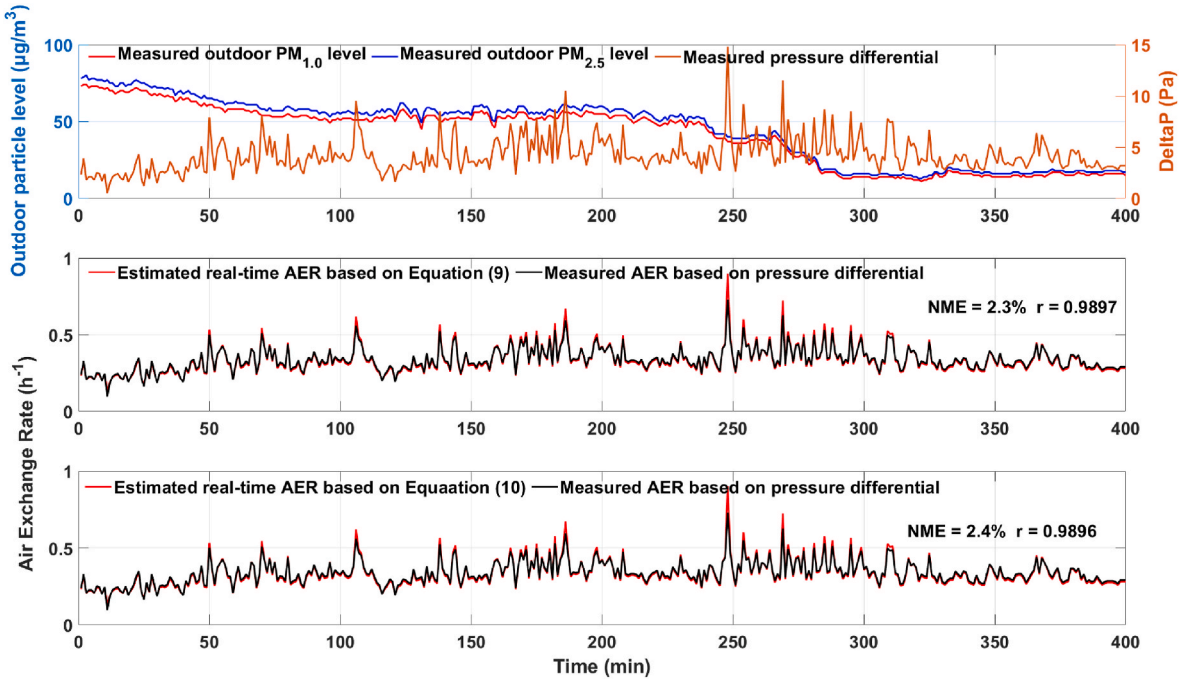

Fig. 13. The comparison of the estimated real-time AER with the measured value.

3.4.1. Accuracy analysis

The additional dataset collected in the previous study was used to verify the empirical correlation and evaluate the accuracy of the numerical model. Equations (9) and (10) were applied to estimate the real-time AER based on measured data obtained during different seasons. Fig. 13 provides a visual representation of the comparison results between the estimated real-time AER and the measured values for a selected day. Table 6 presents a comprehensive comparison of all estimated AER values with the actual AER, using the NME and r as evaluation metrics.

From examining Fig. 13, it is evident that the estimated AER obtained using the established numerical model aligns well with the measured real-time AER. The $PM_{1.0}$-based method yielded an NME of 2.3% and an r value of 0.9879, while the $PM_{2.5}$-based method resulted in an NME of 2.4% and an r value of 0.9896 compared to the actual AER. Table 6 demonstrates that the accuracy of estimating the real-time AER is generally comparable between the $PM_{1.0}$ and $PM_{2.5}$-based methods. This similarity may be attributed to $PM_{1.0}$ being the dominant component of $PM_{2.5}$ in China (Chen et al., 2017; Yang et al., 2020).

Furthermore, Table 6 indicates that the established equation performs well under various outdoor conditions and seasons, even when the outdoor particle level is relatively low, as demonstrated on Day 3 in the spring. Thus, the empirical correlation can be effectively employed to determine the real-time AER based on airborne particles, enabling designers to accurately predict the building's heat loss.

Table 6
Accuracy analysis of the numerical model.

		Average outdoor level (μg/m^3)	Average deltaP (Pa)	NME (%)	r
Winter	$PM_{1.0}$	64.96	2.94	4.37	0.991
Day 1	$PM_{2.5}$	70.46		4.42	0.991
Winter	$PM_{1.0}$	107.10	2.73	7.93	0.980
Day 2	$PM_{2.5}$	117.63		7.87	0.980
Winter	$PM_{1.0}$	38.18	4.92	3.54	0.989
Day 3	$PM_{2.5}$	42.24		3.68	0.989
Spring	$PM_{1.0}$	43.63	4.01	3	0.986
Day 1	$PM_{2.5}$	46.28		3.11	0.986
Spring	$PM_{1.0}$	40.31	4.16	2.3	0.990
Day 2	$PM_{2.5}$	43.59		2.42	0.990
Spring	$PM_{1.0}$	8.10	1.32	7.48	0.976
Day 3	$PM_{2.5}$	9.22		7.04	0.976

3.5. Limitation

In addition to the contributions of this study, some technical limitations are also present to be explored via further research investigation. Firstly, the IPL is also impacted by the deposition and resuspension rate, and these two mechanisms are correlated to human indoor activities. However, this study only concerned the scenario in which the selected room is unoccupied, and thus, further research is required to investigate how human activities disturb the accuracy of using particles as the tracer to measure the AER of a building. An office room was chosen for this analysis based on its air pollution level and the AER's influence. However, since the estimated air pollution levels and air infiltration levels may be different, depending on neighbouring rooms' air pressures and pollution levels, the building's façade opening ratio, ventilation system performance and occupants' behaviour, a further study should carefully consider other elements, such as indoor air pollution sources, air purifier, construction material, wind velocity and direction, and other system facilities. These would be crucial, especially when indoor air quality and occupants' health in buildings are significantly affected by surrounding environments. Also, another parameter may need to be considered for estimating AER during low levels of outdoor particle seasons. Moreover, other actual air contaminant types should be considered to indicate the sources of air contaminants. In a future study, AER could be estimated using other air contaminant sources such as Sulphur Oxides (SOx) and Nitrogen Oxides (NOx), which also come from the surrounding outdoor environment.

4. Conclusion

The study aimed to determine the feasibility of using airborne particles to predict the AER of a building through experiments and numerical simulations. The airtightness of a selected room was determined using the pressurization method, and the measured value was used to assess the real-time AER. The study found that the accuracy of estimating the IPL and predicting the real-time AER was significantly affected by particle size and outdoor conditions. The accuracy of AER estimation based on particles had a negative correlation with particle size, and particles under 2.5 μm were suggested as a tracer to predict the AER since smaller particles have a higher penetration rate. The I/O ratio and pressure differential of particles positively impacted the accuracy of AER estimation, with the I/O ratio having a greater effect than the pressure differential. However, the accuracy of using particle-based methods to estimate AER decreased as the outdoor particle level decreased, though this influence was lessened when the particle size decreased.

The study also established empirical correlations for $PM_{1.0}$ and $PM_{2.5}$ based on experimental data, which were verified using the 5-fold cross-validation method. The correlations proved to be reliable for predicting the real-time AER under various outdoor conditions, and the equation could predict the building's AER based on measured IPL, OPL, and pressure differential. The study suggested using small size particles as a tracer to measure the real-time AER of a high-rise building since the tracer gas method is limited, and the real-time AER could accurately predict the building's heat loss.

Credit author statement

Nuodi Fu: Conceptualization, Methodology, Resources, Software, Writing – original draft, Moon Keun Kim: Conceptualization, Methodology, Writing-reviewing and editing, Supervision, Formal analysis, Validation. Long Huang: Writing – review & editing, Resources, Data curation Jiying Liu: Writing – review & editing, Resources, Investigation. Bing Chen: Writing – review & editing, Supervision, Stephen Sharples: Writing – review & editing, Methodology, Supervision.

Declaration of competing interest

The authors declare that they have no known competing financial interests or personal relationships that could have appeared to influence the work reported in this paper.

Acknowledgement

The author(s) disclosed receipt of the following financial support for the research, authorship, and or publication of this article: This work was supported by the Jiangsu Funding Program for Excellent Postdoctoral Talent, China, the Research Development Fund (RDF 15–02-32 and RDF 20-01-16) of Xi'an Jiaotong - Liverpool University, China, the Department of Built Environment of Oslo Metropolitan University, Norway, the UK ICE Research Development Enabling Fund (ICE-RDF-2020),Natural Science Foundation of Shandong Province (ZR2021ME199), China and the Natural Science Foundation of Zhejiang Province (LY19E080001), China.

References

Amphalop, S., Chienthavorn, O., Meesat, R., Tangpong, P., Chutichaisakda, M., Manohar, M., Wilkins, F., Sudprasert, W., 2023. Source identification of PM2.5 during the COVID-19 lockdown in Bangkok and the metropolitan region by ion beam analysis (IBA) and positive matrix factorization (PMF) techniques. Atmos. Pollut. Res. 14 (7), 101814 https://doi.org/10.1016/j.apr.2023.101814.

Ashrae, I., 2017. 2017 ASHRAE handbook : fundamentals. In: Bibliographies Handbooks Non-fiction Electronic Document, SI edition. ASHRAE. http://app.knovel.com/hotlink/toc/id:kpASHRAEQ1/2017-ashrae-handbook?kpromoter=marc.

ASTM, E, 2000. Standard Test Method for Determining Air Change in a Single Zone by Means of a Tracer Gas Dilution. Proc. ASTM. American Society for Testing and Materials. Standard Test Method for Determining Air Change in a Single Zone by Means of a Tracer Gas Dilution, ASTM International 2000.

Ben-David, T., Waring, M.S., 2016. Impact of natural versus mechanical ventilation on simulated indoor air quality and energy consumption in offices in fourteen U.S. cities. Build. Environ. 104, 320–336. https://doi.org/10.1016/j.buildenv.2016.05.007. Article.

CEN, 2001. *BS EN 13829:2001 Thermal Performance of Buildings. Determination of Air Permeability of Buildings. Fan pressurization Method* [Standards]. BSI Standards Limited. https://search.ebscohost.com/login.aspx?direct=true&db=edsbsi&AN=edsbsi.19983036&site=eds-live&scope=site.

Chen, G., Li, S., Zhang, Y., Zhang, W., Li, D., Wei, X., He, Y., Bell, M.L., Williams, G., Marks, G.B., Jalaludin, B., Abramson, M.J., Guo, Y., 2017. Effects of ambient PM1 air pollution on daily emergency hospital visits in China: an epidemiological study. Lancet Planet. Health 1 (6), e221–e229. https://doi.org/10.1016/S2542-5196(17)30100-6.

CIBSE, 2016. Ventilation and Ductwork. The Chartered Institution of Building Services Engineers, London.

Diapouli, E., Chaloulakou, A., Koutrakis, P., 2013. Estimating the concentration of indoor particles of outdoor origin: a review. J. Air Waste Manag. Assoc. 63 (10), 1113–1129. https://doi.org/10.1080/10962247.2013.791649.

Diapouli, E., Chaloulakou, A., Spyrellis, N., 2007. Indoor and outdoor particulate matter concentrations at schools in the athens area. Indoor Built Environ. 16 (1), 55–61. https://doi.org/10.1177/1420326X06074836.

EPA, 2019. Indoor Particulate Matter _ Indoor Air Quality (IAQ). https://www.epa.gov/indoor-air-quality-iaq/indoor-particulate-matter.

Fattah, M.A., Morshed, S.R., Kafy, A.A., Rahaman, Z.A., Rahman, M.T., 2023. Wavelet coherence analysis of PM2.5 variability in response to meteorological changes in South Asian cities. Atmos. Pollut. Res. 14 (5), 101737 https://doi.org/10.1016/j.apr.2023.101737.

Fu, N., Kim, M.K., Chen, B., Sharples, S., 2021a. Comparative modelling analysis of air pollutants, PM2.5 and energy efficiency using three ventilation strategies in a high-rise building: a case study in Suzhou, China. Sustainability 13 (15), 8453. https://www.mdpi.com/2071-1050/13/15/8453.

Fu, N., Kim, M.K., Chen, B., Sharples, S., 2021b. Investigation of outdoor air pollutant, PM2.5 affecting the indoor air quality in a high-rise building. Indoor Built Environ. 31 (4), 895–912. https://doi.org/10.1177/1420326x211038279.

Fu, Nuodi, Kim, Moon Keun, Huang, Long, Liu, Jiying, Chen, Bing, Sharples, Stephen, 2022. Experimental and numerical analysis of indoor air quality affected by outdoor air particulate levels ($PM_{1.0}$, $PM_{2.5}$ and PM_{10}), room infiltration rate, and occupants' behaviour. Science of The Total Environment 851, 158026. Part 2, 10 December 2022. https://doi.org/10.1016/j.scitotenv.2022.158026.

Gomes, C., Freihaut, J., Bahnfleth, W., 2007. Resuspension of allergen-containing particles under mechanical and aerodynamic disturbances from human walking. Atmos. Environ. 41 (25), 5257–5270. https://doi.org/10.1016/j.atmosenv.2006.07.061.

Goubran, S., Qi, D., Saleh, W.F., Wang, L., 2017. Comparing methods of modeling air infiltration through building entrances and their impact on building energy simulations. Energy Build. 138, 579–590. https://doi.org/10.1016/j.enbuild.2016.12.071.

Han, G., Srebric, J., Enache-Pommer, E., 2015. Different modeling strategies of infiltration rates for an office building to improve accuracy of building energy simulations. Energy Build. 86, 288–295. https://doi.org/10.1016/j.enbuild.2014.10.028.

Happle, G., Fonseca, J.A., Schlueter, A., 2017. Effects of air infiltration modeling approaches in urban building energy demand forecasts. Energy Proc. 122, 283–288. https://doi.org/10.1016/j.egypro.2017.07.323.

He, C., Morawska, L., Gilbert, D., 2005. Particle deposition rates in residential houses. Atmos. Environ. 39 (21), 3891–3899. https://doi.org/10.1016/j.atmosenv.2005.03.016.

Hu, H., Huang, X., Zhao, Y., Qian, H., Liu, C., 2022. A new PM2.5-based PM-up method to measure non-mechanical ventilation rate in buildings. J. Build. Eng. 52, 104351 https://doi.org/10.1016/j.jobe.2022.104351.

Hu, Y., Yao, M., Liu, Y., Zhao, B., 2020. Personal exposure to ambient PM2.5, PM10, O3, NO2, and SO2 for different populations in 31 Chinese provinces. Environ. Int. 144, 106018 https://doi.org/10.1016/j.envint.2020.106018.

Huang, W., Xie, X., Qi, X., Huang, J., Li, F., 2017. Determination of particle penetration coefficient, particle deposition rate and air infiltration rate in classrooms based on monitored indoor and outdoor concentration levels of particle and carbon dioxide. Procedia Eng. 205, 3123–3129. https://doi.org/10.1016/j.proeng.2017.10.126.

Isiugo, K., Jandarov, R., Cox, J., Chillrud, S., Grinshpun, S.A., Hyttinen, M., Yermakov, M., Wang, J., Ross, J., Reponen, T., 2019. Predicting indoor concentrations of black carbon in residential environments. Atmos. Environ. 201, 223–230. https://doi.org/10.1016/j.atmosenv.2018.12.053.

ISO, 2012. 12569: 2012: Thermal Performance of Buildings and Materials-Determination of Specific Airflow Rate in Buildings-Tracer Gas Dilution Method. In: ISO %J International Organization for Standardization.

Ji, Y., Duanmu, L., 2017a. Air-tightness test and air infiltration estimation of an ultra-low energy building. Sci. Technol. Built Environ. 23 (3), 441–448. https://doi.org/10.1080/23744731.2017.1262707.

Ji, Y., Duanmu, L., 2017b. Airtightness field tests of residential buildings in Dalian, China. Build. Environ. 119, 20–30. https://doi.org/10.1016/j.buildenv.2017.03.043.

Ji, Y., Duanmu, L., Li, X., 2017. Building air leakage analysis for individual apartments in North China. Build. Environ. 122, 105–115. https://doi.org/10.1016/j.buildenv.2017.06.007.

Ji, Y., Duanmu, L., Liu, Y., Dong, H., 2020. Air infiltration rate of typical zones of public buildings under natural conditions. Sustain. Cities Soc. 61, 102290 https://doi.org/10.1016/j.scs.2020.102290.

Kabirikopaei, A., Lau, J., 2020. Uncertainty analysis of various CO2-Based tracer-gas methods for estimating seasonal ventilation rates in classrooms with different mechanical systems. Build. Environ. 179, 107003 https://doi.org/10.1016/j.buildenv.2020.107003.

Kim, M.K., Choi, J.-H., 2019. Can increased outdoor CO2 concentrations impact on the ventilation and energy in buildings? A case study in Shanghai, China. Atmos. Environ. 210, 220–230. https://doi.org/10.1016/j.atmosenv.2019.04.015.

Kim, M.K., Cremers, B., Liu, J., Zhang, J., Wang, J., 2022. Prediction and correlation analysis of ventilation performance in a residential building using artificial neural network models based on data-driven analysis [Article]. Sustain. Cities Soc. 83, 103981 https://doi.org/10.1016/j.scs.2022.103981.

Lai, A.C., Nazaroff, W.W., 2000. Modeling indoor particle deposition from turbulent flow onto smooth surfaces. J. Aerosol Sci. 31 (4), 463–476. J. J. o. a. s.

Lee, S., Cheng, Y., Ho, K.F., Cao, J., Louie, P.K.K., Chow, J., Watson, J., 2006. PM 1.0 and PM 2.5 characteristics in the roadside environment of Hong Kong. Aerosol. Sci. Technol. 40, 157–165. https://doi.org/10.1080/02786820500494544.

Li, G., Chen, L., Yang, H., 2022. Prediction of PM2.5 concentration based on improved secondary decomposition and CSA-KELM. Atmos. Pollut. Res. 13 (7), 101455 https://doi.org/10.1016/j.apr.2022.101455.

Li, N., Liu, Z., Li, Y., Li, N., Chartier, R., McWilliams, A., Chang, J., Wang, Q., Wu, Y., Xu, C., Xu, D., 2019. Estimation of PM2.5 infiltration factors and personal exposure factors in two megacities, China. Build. Environ. 149, 297–304. https://doi.org/10.1016/j.buildenv.2018.12.033.

Liang, D., Lee, W.-C., Liao, J., Lawrence, J., Wolfson, J.M., Ebelt, S.T., Kang, C.-M., Koutrakis, P., Sarnat, J.A., 2021. Estimating climate change-related impacts on outdoor air pollution infiltration. Environ. Res. 196, 110923 https://doi.org/10.1016/j.envres.2021.110923.

Liu, C., Ji, S., Zhou, F., Lin, Q., Chen, Y., Shao, X., 2021. A new PM2.5-based CADR method to measure air infiltration rate of buildings. Build. Simulat. 14 (3), 693–700. https://doi.org/10.1007/s12273-020-0676-4.

Liu, F., Zheng, X.H., Qian, H., 2018. Comparison of particle concentration vertical profiles between downtown and urban forest park in Nanjing (China). Atmos. Pollut. Res. 9 (5), 829–839. https://doi.org/10.1016/j.apr.2018.02.001.

Martins, N.R., Carrilho da Graça, G., 2018. Impact of PM2.5 in indoor urban environments: a review. Sustain. Cities Soc. 42, 259–275. https://doi.org/10.1016/j.scs.2018.07.011.

Mathur, U., Damle, R., 2021. Impact of air infiltration rate on the thermal transmittance value of building envelope. J. Build. Eng. 40, 102302 https://doi.org/10.1016/j.jobe.2021.102302.

Meng, Q.Y., Turpin, B.J., Polidori, A., Lee, J.H., Weisel, C., Morandi, M., Colome, S., Stock, T., Winer, A., Zhang, J., 2005. PM2.5 of ambient origin: estimates and exposure errors relevant to PM epidemiology. Environ. Sci. Technol. 39 (14), 5105–5112. https://doi.org/10.1021/es048226f.

Nazaroff, W.W., 2021. Residential air-change rates: a critical review. Indoor Air 31 (2), 282–313. https://doi.org/10.1111/ina.12785, 10.1111/ina.12785.

Ni, P., Jin, H.C., Wang, X.l., Xi, G., 2017. A new method for measurement of air change rate based on indoor PM2.5 removal. Int. J. Environ. Sci. Technol. 15, 2561–2568. J. I. J. o. E. S., & Technology.

Park, S., Choi, P., Song, D., Koo, J., 2021. Estimation of the real-time infiltration rate using a low carbon dioxide concentration. J. Build. Eng. 42, 102835 https://doi.org/10.1016/j.jobe.2021.102835.

Qian, J., Ferro, A.R., 2008. Resuspension of dust particles in a chamber and associated environmental factors. Aerosol. Sci. Technol. 42 (7), 566–578. https://doi.org/10.1080/02786820802220274.

Quang, T.N., He, C., Morawska, L., Knibbs, L.D., 2013. Influence of ventilation and filtration on indoor particle concentrations in urban office buildings. Atmos. Environ. 79, 41–52. https://doi.org/10.1016/j.atmosenv.2013.06.009.

Ren, C., Chen, H.F., Wang, J.Q., Feng, Z.B., Cao, S.J., 2022. Ventilation impacts on infection risk mitigation, improvement of environmental quality and energy efficiency for subway carriages. Build. Environ. 222, 109358 https://doi.org/10.1016/j.buildenv.2022.109358.

Ren, C., Wang, J.Q., Feng, Z.B., Kim, M.K., Haghighat, F., Cao, S.J., 2023a. Refined design of ventilation systems to mitigate infection risk in hospital wards: perspective from ventilation openings setting. Environ. Pollut. 333, 122025 https://doi.org/10.1016/j.envpol.2023.122025.

Ren, C., Zhu, H.C., Wang, J.Q., Feng, Z.B., Chen, G., Haghighat, F., Cao, S.J., 2023b. Intelligent operation, maintenance, and control system for public building: towards infection risk mitigation and energy efficiency. Sustain. Cities Soc. 93, 104533 https://doi.org/10.1016/j.scs.2023.104533.

Ren, L., An, F., Su, M., Liu, J., 2022. Exposure assessment of traffic-related air pollution based on CFD and BP neural network and artificial intelligence prediction of optimal route in an urban area [article]. Buildings 12 (8), 1227. https://doi.org/10.3390/buildings12081227.

Rojas-Bracho, L., Suh, H.H., Catalano, P.J., Koutrakis, P., 2004. Personal exposures to particles and their relationships with personal activities for chronic obstructive pulmonary disease patients living in Boston. J. Air Waste Manag. Assoc. 54 (2), 207–217. https://doi.org/10.1080/10473289.2004.10470897.

Ruan, T., Rim, D., 2019. Indoor air pollution in office buildings in mega-cities: effects of filtration efficiency and outdoor air ventilation rates. Sustain. Cities Soc. 49, 101609 https://doi.org/10.1016/j.scs.2019.101609.

Serfozo, N., Chatoutsidou, S.E., Lazaridis, M., 2014. The effect of particle resuspension during walking activity to PM10 mass and number concentrations in an indoor microenvironment. Build. Environ. 82, 180–189. https://doi.org/10.1016/j.buildenv.2014.08.017.

Shi, Y., Li, X., 2018a. Purifier or fresh air unit? A study on indoor particulate matter purification strategies for buildings with split air-conditioners. Build. Environ. 131, 1–11. https://doi.org/10.1016/j.buildenv.2017.12.033.

Shi, Y., Li, X., 2018b. A study on variation laws of infiltration rate with mechanical ventilation rate in a room. Build. Environ. 143, 269–279. https://doi.org/10.1016/j.buildenv.2018.07.021.

Shi, Y., Li, X., Li, H., 2017. A new method to assess infiltration rates in large shopping centers. Build. Environ. 119, 140–152. https://doi.org/10.1016/j.buildenv.2017.04.011.

Stamp, S., Burman, E., Chatzidiakou, L., Cooper, E., Wang, Y., Mumovic, D., 2022. A critical evaluation of the dynamic nature of indoor-outdoor air quality ratios. Atmos. Environ. 273, 118955 https://doi.org/10.1016/j.atmosenv.2022.118955.

Stratigou, E., Dusanter, S., Brito, J., Riffault, V., 2020. Investigation of PM10, PM2.5, PM1 in an unoccupied airflow-controlled room: how reliable to neglect resuspension and assume unreactive particles? Build. Environ. 186, 107357 https://doi.org/10.1016/j.buildenv.2020.107357.

Sun, Z., Liu, C., Zhang, Y., 2019. Evaluation of a steady-state method to estimate indoor PM2.5 concentration of outdoor origin. Build. Environ. 161, 106243 https://doi.org/10.1016/j.buildenv.2019.106243.

Wang, H.R., Wang, J.Q., Feng, Z.B., Haghighat, F., Cao, S.J., 2023. An intelligent anti-infection ventilation strategy: from occupant-centric control and computer vision perspectives. Energy Build. 296, 113403 https://doi.org/10.1016/j.enbuild.2023.113403.

Wichmann, J., Lind, T., Nilsson, M.A.M., Bellander, T., 2010. PM2.5, soot and NO2 indoor–outdoor relationships at homes, pre-schools and schools in Stockholm, Sweden. Atmos. Environ. 44 (36), 4536–4544. https://doi.org/10.1016/j.atmosenv.2010.08.023.

Wu, Y., Hao, J.M., Fu, L.X., Wang, Z.S., Tang, U., 2002. Vertical and horizontal profiles of airborne particulate matter near major roads in Macao, China. Atmos. Environ. 36

(31), 4907–4918. https://doi.org/10.1016/S1352-2310(02)00467-3. Pii S1352-2310(02)00467-3.
Xiang, J., Huang, C.-H., Shirai, J., Liu, Y., Carmona, N., Zuidema, C., Austin, E., Gould, T., Larson, T., Seto, E., 2021. Field measurements of PM2.5 infiltration factor and portable air cleaner effectiveness during wildfire episodes in US residences. Sci. Total Environ. 773, 145642 https://doi.org/10.1016/j.scitotenv.2021.145642.
Xiong, Z., Berquist, J., Gunay, H.B., Cruickshank, C.A., 2021. An inquiry into the use of indoor CO2 and humidity ratio trend data with inverse modelling to estimate air infiltration. Build. Environ. 206, 108365 https://doi.org/10.1016/j.buildenv.2021.108365.
Yang, J., Nam, I., Yun, H., Kim, J., Oh, H.-J., Lee, D., Jeon, S.-M., Yoo, S.-H., Sohn, J.-R., 2015. Characteristics of indoor air quality at urban elementary schools in Seoul, Korea: assessment of effect of surrounding environments. Atmos. Pollut. Res. 6 (6), 1113–1122. https://doi.org/10.1016/j.apr.2015.06.009.
Yang, M., Guo, Y.-M., Bloom, M.S., Dharmagee, S.C., Morawska, L., Heinrich, J., Jalaludin, B., Markevychd, I., Knibbsf, L.D., Lin, S., Hung Lan, S., Jalava, P., Komppula, M., Roponen, M., Hirvonen, M.-R., Guan, Q.-H., Liang, Z.-M., Yu, H.-Y., Hu, L.-W., Yang, B.-Y., Zeng, X.-W., Dong, G.-H., 2020. Is PM1 similar to PM2.5? A new insight into the association of PM1 and PM2.5 with children's lung function. Environ. Int. 145, 106092 https://doi.org/10.1016/j.envint.2020.106092.
Yu, C.K.H., Li, M., Chan, V., Lai, A.C.K., 2014. Influence of mechanical ventilation system on indoor carbon dioxide and particulate matter concentration. Build. Environ. 76, 73–80. https://doi.org/10.1016/j.buildenv.2014.03.004.
Zhao, B., Wu, J., 2007. Particle deposition in indoor environments: analysis of influencing factors. J. Hazard Mater. 147 (1), 439–448. https://doi.org/10.1016/j.jhazmat.2007.01.032.
Zong, J., Liu, J., Ai, Z., Kim, M.K., 2022. A review of human thermal plume and its influence on the inhalation exposure to particulate matter. Indoor Built Environ. 31 (7), 1758–1774. https://doi.org/10.1177/1420326X221080358 submitted for publication.